Food Chemistry 181 (2015) 43–50

Contents lists available at ScienceDirect

Food Chemistry

journal homepage: www.elsevier.com/locate/foodchem

Molecular order and functional properties of starches from three waxy wheat varieties grown in China

Shujun Wang [a,*], Jinrong Wang [a], Wei Zhang [a], Caili Li [a], Jinglin Yu [b], Shuo Wang [a,*]

[a] Key Laboratory of Food Nutrition and Safety, Ministry of Education, College of Food Engineering and Biotechnology, Tianjin University of Science & Technology, Tianjin 300457, China
[b] Research Centre of Modern Analytical Technique, Tianjin University of Science & Technology, Tianjin 300457, China

ARTICLE INFO

Article history:
Received 4 December 2014
Received in revised form 12 February 2015
Accepted 13 February 2015
Available online 20 February 2015

Keywords:
Waxy wheat starch
Crystallinity
FTIR spectroscopy
Raman spectroscopy
Pasting
Retrogradation

ABSTRACT

Molecular order and functional properties of starch from three waxy wheat varieties grown in China were investigated by a combination of various technical analyses. The total starch content of the waxy wheat ranged between 54.1% and 55.0%, and the amylose content of the starch was between 0.71% and 1.63%. Average particle diameter of the three starches varied between 16.5 and 17.4 μm. Three waxy wheat starches presented the typical A-type X-ray diffraction pattern, with relative crystallinity between 38.7% and 40.0%. No significant differences were observed in relative crystallinity, IR ratios of 1047/1022 cm^{-1} and 1022/995 cm^{-1}, and FWHH of the band at 480 cm^{-1}, indicating the similarity in long-range order of crystallites and short-range order of double helices of three starch granules. Small differences were observed in swelling power, gelatinization parameters, pasting viscosities, and *in vitro* enzymatic digestibility of three waxy wheat starches. Under the stored condition, no retrogradation occurred for three waxy wheat starches.

1. Introduction

Wheat, one of the oldest crops, is widely cultivated in many countries around the world. As a major staple food, wheat is consumed in various forms such as breads, noodles and other baked or steamed products by over one-third of the global population. Wheat is one of the top three most produced crops in the world, along with maize and rice (Kumar & Prabhasankar, 2014). According to the report of Food and Agricultural Organization (FAO), the world total production of wheat has reached 660 million tons in 2012, of which one-fifth (126 million tons) is produced in China. China is not only the largest wheat producer, but also the biggest wheat consumer in the world. Common or wild-type wheat has been cultivated for over 10,000 years, and in China, it has been 4000–5000 years for wheat cultivation (Dodson et al., 2013). In contrast to common wheat, completely waxy wheat was first developed by traditional hybridizations in 1995 (Nakamura, Yamamori, Hirano, Hidaka, & Nagamine, 1995). Since then, waxy wheat has been successively produced in Australia, USA and Canada (Zhang, Zhang, Xu, & Zhou, 2013). In 2005, the Chinese famous wheat breeding expert Shunhe Cheng developed a completely waxy wheat variety. In last 5 years, several new waxy wheat varieties have been produced in China and their application in foods has been explored (Ma et al., 2013).

Wheat grains are mainly composed of starch and protein, which account for about 50–60% and 8–20% of the dry weight grain, respectively. Protein, especially gluten, plays an important role in the rheological properties of the mixed dough and the textural properties of the finished food products (Goesaert et al., 2005). In contrast, starch makes diverse contributions to control of moisture, viscosity, texture, consistency, mouth-feel, shelf life and nutrition of the starch-based foods (Wang & Copeland, 2013). The extent of starch contribution to food quality and nutrition mainly rely on the functionality of starch in the presence of water, which refers to swelling power, solubility, gelatinization, pasting, retrogradation and susceptibility to enzymatic digestion. The high variability in native starch functionality derives from variability of structure, which is due to diversity in the genes that encode the starch biosynthetic enzymes and environmental factors that act on the genes and enzymes concerned during plant growth (Wang & Copeland, 2015). Waxy wheat starch, which is biosynthesized when the three granule-bound starch synthesis (GBSS) genes are absent or nonfunctional, has distinct structural characteristics such as very low amylose content and high crystallinity. These structural characteristics endow waxy wheat starch the desirable functional properties such as high swelling power and peak viscosity, low retrogradation, setback viscosity and pasting temperature

* Corresponding authors.
E-mail addresses: sjwang@tust.edu.cn (S. Wang), s.wang@tust.edu.cn (S. Wang).

http://dx.doi.org/10.1016/j.foodchem.2015.02.065
0308-8146/

(Hung, Maeda, & Morita, 2006). These desirable functional properties make waxy wheat starch highly potential in replacing the normal wheat starch in food products (Hung et al., 2006; Ma et al., 2013).

With the increasing development of new waxy wheat varieties, the comprehensive understanding of starch structure and functionality in waxy wheat grains is extremely important for their appropriate application in foods. There have been some studies regarding the characterization of waxy wheat starch (Chakraboty et al., 2004; Fujita, Yamamoto, Sugimoto, Morita, & Yamamori, 1998; Kim & Huber, 2010; Yoo & Jane, 2002; Zhang et al., 2013). However, little information is available for starches from waxy wheat grown in China. Moreover, the short-range molecular order of waxy wheat starches as measured by FTIR and Raman spectroscopy, and their relationship with the long-range order (crystallinity) were not well understood. In the present study, three waxy wheat varieties (Ning Waxy1-NW1, Tian Waxy1-TW1, and Yang Waxy1-YW1) developed in China were obtained for the comprehensive characterization of starch molecular order and functionality. For the first time, the short-range molecular order of three waxy wheat starches is fully characterized by Fourier transform infrared (FTIR) and laser confocal micro-Raman (LCM-Raman) spectroscopy. The relationship between molecular order and starch crystallinity is also investigated.

2. Materials and methods

2.1. Materials

Three waxy wheat grains were kindly provided by Lixiahe Agricultural Research Institute, Jiangsu Province, China. Wheat grains were harvested in the 2012–2013 season. Total starch assay kit, glucose oxidase/peroxidase (GOPOD) kit and amyloglucosidase (3260 U/ml) were purchased from Megazyme International Ireland Ltd. (Bray Co., Vicklow, Ireland). Amylose (A0512) and amylopectin (A8515) from potato starch, and α-amylase (Sigma, EC 3.2.1.1, type VI-B from porcine pancreas, 28 U/mg) were purchased from Sigma Chemical Co. (St. Louis, MO, USA). Other chemical reagents were of all analytical grade.

2.2. Isolation of starch

Starch was isolated from waxy wheat grains according to the method of Wang, Hassani, Crossett, and Copeland (2013) with minor modifications as follows. Wheat grains (250 g) were soaked in 1 L of ammonia solution (0.2 M) for 24 h at room temperature. The supernatant was decanted and the softened grains were blended in a kitchen blender with ammonia solution (wheat/ammonium: 1/6 (w/v)) for 1–2 min. The resulting slurry was filtered through a 250 μm nylon mesh (filtrate 1). The residue was mixed with ammonia solution, blended and filtered through a 250 μm nylon mesh (filtrate 2). The combined filtrate 1 and filtrate 2 was centrifuged at 3500*g* for 15 min and the supernatant was decanted. The top layer of sedimented starch (SS1) was resuspended in ammonia solution and centrifuged at 5000*g* for 10 min. The top layer of the sedimented starch (SS2) was scrapped off. The combined SS1 and SS2 was resuspended in ammonia solution and centrifuged at 5000*g* for 10 min. This process was repeated for three times. After centrifugation, the sedimented starch was suspended in water and centrifuged at 5000*g* for 10 min. The starch precipitate was blended in 0.2 M acetic acid solution and filtered through a 120 μm nylon mesh. The filtrate was centrifuged at 5000*g* for 10 min and the crude starch was obtained. The crude starch was washed with distilled water for three times and then washed with ethanol twice. The resulting starch was dried in air condition and then stored in a container at 4 °C.

2.3. Chemical composition of wheat grains and isolated starches

Dry wheat grains were milled into flour and passed through a 250 μm sieve. The resulting flour was used for the determination of total starch and protein content of wheat. Total starch content of wheat was determined by Megazyme total starch assay kit. The nitrogen content of wheat grains and starch granules were determined by standard Kjeldahl methodology. Protein content was estimated by multiplying the nitrogen content by a conversion factor of 6.25. Apparent amylose content of the wheat starches was determined by the iodine binding method of Chrastil (1987) using a standard curve of 0%, 5%, 10%, 20%, 25% and 30% potato amylose mixed with potato amylopectin. The lipid content of starch granules was determined gravimetrically after extraction with ether at 60–70 °C for 12 h. Moisture content was determined by oven drying of the starch at 105 °C until constant weight.

2.4. Granule morphology

The morphology of starch granules was imaged using a SU1510 scanning electron microscope (Hitachi High-technologies Corporation, Japan). Starch samples were mounted on the aluminum stub using double-sided carbon adhesive tape and sputter-coated with gold. An accelerating voltage of 5 kV was used during imaging.

2.5. Granule size distribution

Size distribution of starch granules was determined using a BT-9300S laser particle size analyzer (Dandong Bettersize Instruments Ltd., Dandong, China). The starch was dispersed in distilled water with magnetic agitation to attain an obscuration of about 12%. All measurements were performed in triplicate and the median volume-based diameter was used to represent the average granule size.

2.6. X-ray diffraction (XRD)

X-ray diffraction analysis was performed using a D/max-2500vk/pc X-ray diffractometer (Rigaku Corporation, Tokyo, Japan) operating at 40 kV and 30 mA. Starches were equilibrated over a saturated sodium chloride (NaCl) solution at room temperature for one week before analysis (Wang, Yu, Zhu, Yu, & Jin, 2009). The intensity was measured from 5° to 35° as a function of 2θ and at a scanning speed of 1°/min and a step size of 0.02°. The relative crystallinity was quantitatively estimated as a ratio of the crystalline area to the total area between 5° and 35° (2θ) using the Origin software (Version 7.5, Microcal Inc., Northampton, MA, USA).

2.7. Fourier transform infrared (FTIR) spectroscopy

The FTIR spectra of three waxy wheat starches were obtained using a Tensor 27 FTIR spectrometer (Bruker, Germany) equipped with a DLATGS detector. The sample preparation and operation conditions were described elsewhere (Wang, Luo et al., 2014). The ratios of absorbance at 1045/1022 cm^{-1} and 1022/995 cm^{-1} were used to estimate the short-range ordered structure of starch.

2.8. Laser confocal micro-raman (LCM-Raman) spectroscopy

A Renishaw Invia Raman microscope system (Renishaw, Gloucestershire, United Kingdom) equipped with a Leica microscope (Leica Biosystems, Wetzlar, Germany) and a 785 nm green diode laser source was used in this study. Spectra were taken from the same spot size of each sample in the range of 3200–100 cm^{-1},

with a resolution of approximately 7 cm^{-1}. The full width at half height (FWHH) of the band at 480 cm^{-1} was calculated by using the software of WiRE 2.0.

2.9. Swelling power

The swelling power of starch granules was measured at temperatures ranging from 50 to 90 °C according to the method of Wang and Copeland (2012a). The water/starch ratio used in the swelling power test was 25:1, namely 1 ml water/40 mg starch. Starch swelling power was calculated as the ratio of the weight of the sedimented swollen starch to the initial dry weight of starch.

2.10. Differential scanning calorimetry

Differential scanning calorimetry (DSC) measurements were performed using a differential scanning calorimeter (200 F3, Netzsch, Germany) equipped with a thermal analysis data station. Approximately 3 mg of starch were accurately weighed into an aluminum sample pan. Distilled water was added with a pipette to obtain a starch:water ratio of 1:3 (w/v) in the DSC pans. The pans were sealed and allowed to stand overnight at room temperature before analysis. The pans were heated from 20 to 120 °C at a heating rate of 10 °C/min. An empty aluminum pan was used as the reference. The onset (T_o), peak (T_p), conclusion (T_c) temperatures and enthalpy of gelatinization (ΔH_{gel}) were obtained through data recording software. All measurements were performed in triplicate. Starch retrogradation was determined by using the same gelatinized samples. The gelatinized waxy wheat starch were stored at 4 °C for 5 days, rescanned using DSC at the same heating conditions as described above for starch gelatinization.

2.11. Pasting properties

The pasting profiles were monitored using a Rapid Visco Analyser (RVA-4) (Newport Scientific, Warriewood, Australia) according to the procedure described elsewhere (Wang, Sharp, & Copeland, 2011). Starch slurries (8%, db, 28 g total weight) were used for the determination of pasting properties. From RVA profiles, peak viscosity (PV), trough viscosity (TV), final viscosity (FV), and pasting temperature (PT) were obtained. The breakdown (BD, which is PV minus TV) and setback (SB, which is FV minus TV) were calculated using the Thermocline software provided with the instrument. All measurements were done in triplicate.

2.12. In vitro enzymatic digestibility

In vitro starch digestibility was determined by a procedure described in Wang, Luo, et al. (2014). After digestion at specified time points, the concentration of glucose in the digestion solution was measured using the Megazyme GOPOD kit. The kinetic curves of starch digestion were obtained by plotting the percentage of starch digestion as a function of hydrolysis time. Starch classifications based on the rate of hydrolysis were: rapidly digested starch (RDS, digested within 20 min), slowly digested starch (SDS, digested between 20 and 120 min) and resistant starch (RS, undigested starch after 120 min).

2.13. Statistical analysis

Results were reported as the mean values and standard deviations of at least duplicate measurements. Analysis of variance (ANOVA) by Duncan's test ($p < 0.05$) were conducted using the SPSS 10.0 Statistical Software Program (SPSS Inc. Chicago, IL, USA).

3. Results and discussion

3.1. Basic composition of wheat grains and starches

Total starch content of three waxy wheat grains was about 54.1–55.0% (Table 1). No statistically significant differences were observed between varieties. The protein content of waxy wheat grains varied from 13.7% for YW1 to 15.2% for NW1 (Table 1). The amylose content of three waxy wheat starches ranged from 0.71% for TW1 starch to 1.63% for NW1 starch (Table 1), which was comparable to that of usually reported for waxy wheat starch (Chakraboty et al., 2004; Kim & Huber, 2010; Salman et al., 2009; Yoo & Jane, 2002). The lipid content, protein content and moisture content of three waxy wheat starches were in the range of 0.15–0.30%, 0.15–0.25%, and 8.9–10.2%, respectively. The lipid content and protein content were lower than those reported for normal wheat starch Wang, Luo et al., 2014.

3.2. Granule morphology and granule size distribution

Native waxy wheat starch was observed to be composed of two different populations of granules, namely large disk-like granules (A-type) and small spherical granules (B-type) (Fig. 1). Surface of most starch granules was smooth with grooves or indentations being visible on some large granules. Similar observations were also made with starches from normal wheat or other waxy wheat varieties (Chakraboty et al., 2004; Fujita et al., 1998; Kim & Huber, 2010; Salman et al., 2009; Wang, Luo et al., 2014; Wang et al., 2013; Yoo & Jane, 2002; Zhang et al., 2013). The observed grooves or indentations on large A-type granules are likely to be the results of impressions from B-granules or protein bodies during the development of wheat grains. Additionally, a few tiny pores can be seen on the surface of some starch granules, which have also been found in other studies (Fannon, Hauber, & BeMiller, 1992; Wang, Luo et al., 2014; Wang et al., 2013). No significant differences in granular morphology were noted between starches from three waxy wheat varieties. Three waxy wheat starches showed the similar bimodal particle size distribution pattern (data not shown). The mean granule size of three waxy wheat starches ranged from 16.5 μm for NW1 to 17.4 μm for YN1 (Table 1), which was much larger than those reported for starch from Australian waxy wheat varieties in our previous study (Wang et al., 2013). As compared

Table 1
Chemical composition of waxy wheat grains and isolated starches.

Varieties	Wheat grain		Isolated starch				
	TS (%)	Protein (%)	AM (%)	Lipid (%)	Protein (%)	Moisture (%)	MGS (μm)
NW1	54.7 ± 0.7a	15.2 ± 0.5b	1.63 ± 0.16b	0.15 ± 0.04a	0.19 ± 0.09a	9.3 ± 0.1b	16.5 ± 0.4a
TW1	54.1 ± 2.7a	14.1 ± 0.6ab	0.71 ± 0.04a	0.30 ± 0.02b	0.25 ± 0.05a	10.2 ± 0.1c	17.1 ± 0.3ab
YW1	55.0 ± 0.2a	13.7 ± 0.8a	0.82 ± 0.15a	0.24 ± 0.03ab	0.15 ± 0.07a	8.9 ± 0.2a	17.4 ± 0.3b

Values are means ± SD. Means with similar letters in a column do not differ significantly ($p > 0.05$).
TS: total starch; AM: amylose; MGS: mean granule size.

with normal wheat starch, waxy wheat starch granules were generally smaller (Yu et al., 2015).

3.3. Crystallinity of waxy wheat starches

Starches from three waxy wheat varieties presented the similar characteristic diffraction peaks at 2θ 15.4° (singlet), 17–18° (doublet) and 23.1° (singlet), indicating the presence of A-type polymorphs in waxy wheat starches (Fig. 2A). The relative crystallinity of three waxy wheat starches was 38.7%, 39.6% and 40.0% for NW1, TW1 and YW1, respectively. No significant differences were noted between waxy wheat starches. The values of relative crystallinity were similar with those reported previously (Fujita et al., 1998; Zhang et al., 2013). The relative crystallinity of waxy wheat starch is generally higher than that of normal wheat starch. Starch crystallites are assumed to be formed by the regular array of double helices that are formed by the singly branched and unbranched amylopectin side chains with more than 10 glucose units (Gidley, 1987). In comparison with normal starch, waxy starch has more amylopectin molecules, and in turn more side chains with appropriate glucose units to form double helices, which accounts for the higher relative crystallinity.

3.4. FTIR spectra of waxy wheat starches

The FTIR spectra of three waxy wheat starches are presented in Fig. 2B. The characteristic peaks at 3381 and 2934 cm^{-1} were attributed to the vibration of O–H stretching and the C–H deformation of the glucose unit, respectively. The absorbance at 1649 cm^{-1} was associated with the bending vibration of O–H of water absorbed in the amorphous regions of starch. Three characteristic peaks assigned to the vibration of C–O stretching were observed between 1019 and 1162 cm^{-1}. The peaks at 1019 and 1080 cm^{-1} were ascribed to the vibration of C-H and C-O-H bending, respectively. The band at 1162 cm^{-1} was assigned to the vibration of C–O and C–C stretching of anhydroglucose ring (Kizil, Irudayaraj, & Seetharaman, 2002). No clear differences were noted in the FTIR spectra of three waxy wheat starches.

To investigate the short-range molecular order of three waxy wheat starches, the deconvoluted FTIR spectra in the 1200–800 cm^{-1} range of three waxy wheat starches were obtained (Fig. 2C). FTIR has been shown to be sensitive to changes in structure on a molecular level (short-range order) and the IR bands at 1047 and 1022 cm^{-1} have been shown to be associated with ordered and amorphous structures of starch, respectively. The absorbance ratios of 1047/1022 cm^{-1} and 1022/995 cm^{-1} can be used as the indexes of the short-range order of double helices (Sevenou, Hill, Farhat, & Mitchell, 2002; Shingel, 2002; Smits, Ruhnau, Wliegenthart, & van Soest, 1998). The higher relative crystallinity, the higher absorbance ratio of 1047/1022 cm^{-1} and the lower absorbance ratio of 1022/995 cm^{-1}, the higher molecular order of double helices of starch granules (Man et al., 2012; Sevenou et al., 2002). No significant differences between starches were observed in the ratios of 1047/1022 cm^{-1} and 1022/995 cm^{-1} (Table 2), indicating that the short-range molecular order of three waxy wheat starches were similar. This observation was consistent with the results of XRD.

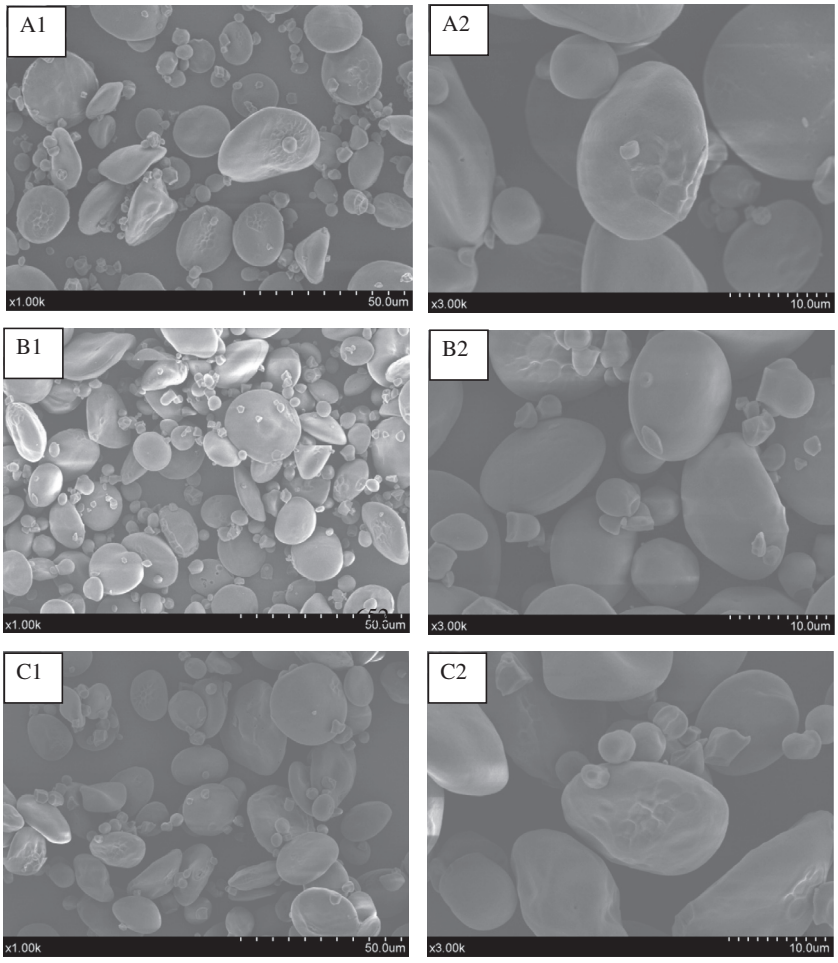

Fig. 1. SEM micrographs of three waxy wheat starches. (A1 and A2) NW1; (B1 and B2) TW1; (C1 and C2) YW1.

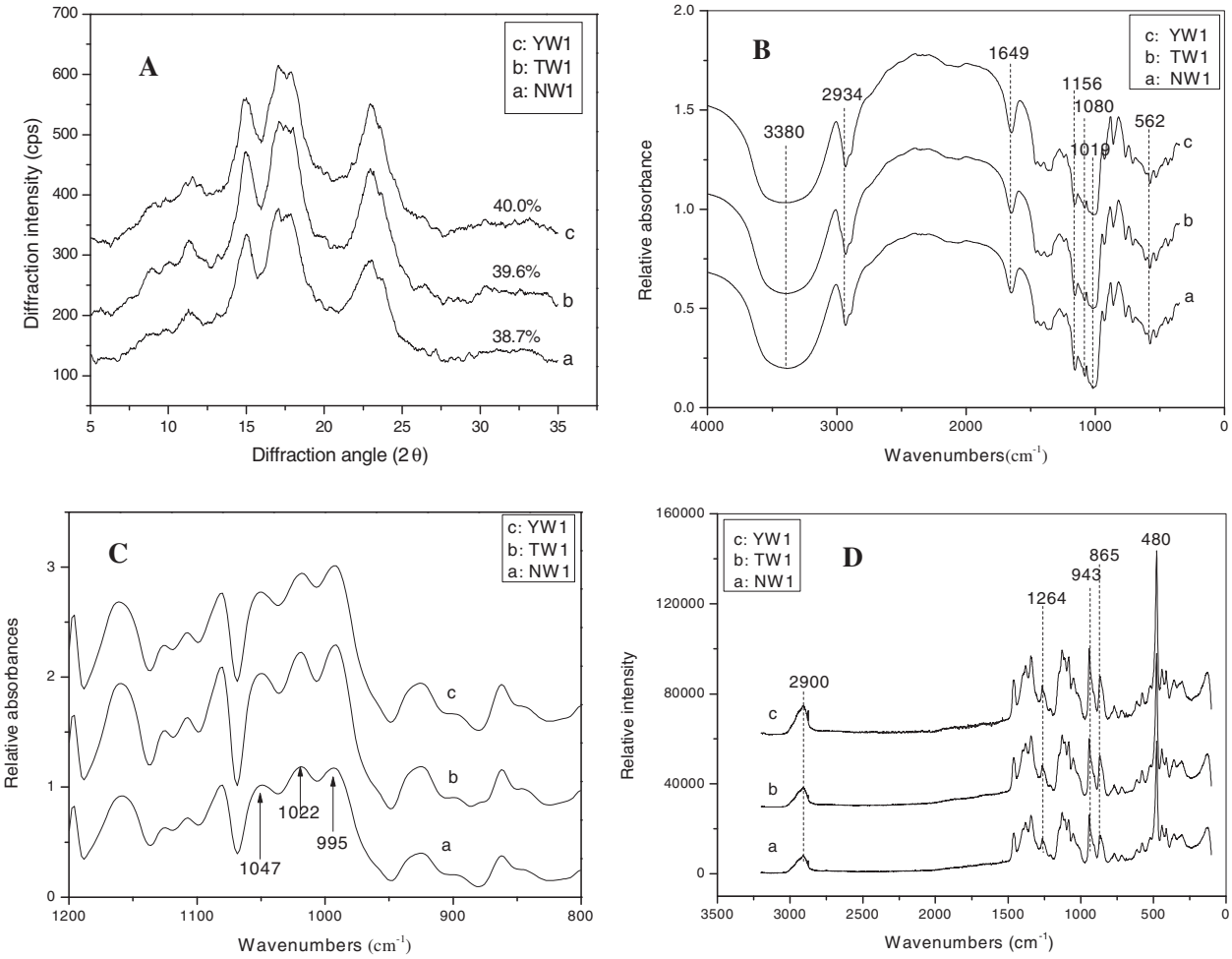

Fig. 2. X-ray diffraction patterns, FTIR spectroscopy and Raman spectroscopy of three waxy wheat starches. (A) X-ray diffraction pattern; (B) FTIR spectroscopy; (C) deconvoluted FTIR spectroscopy from 800 to 1200 cm^{-1}; (D) Raman spectroscopy.

3.5. LCM-Raman spectra of waxy wheat starches

The LCM-Raman spectra of three waxy wheat starches are presented in Fig. 2D. Several clear bands can be seen at 480, 865, 943, 1264 and 2900 cm^{-1}, which are related to δ (CH2), ν_s (C1–O–C4), ν_s (C1–O–C5), skeletal (C–C–O), and ν (C–H) modes, respectively (Mutungi, Passauer, Onyango, Jaros, & Rohm, 2012). Of these bands, the bands at 480 and 2900 cm^{-1} are often used to characterize the molecular order of native starch granules or the changes in molecular order of starch samples during gelatinization or retrogradation (Flores-Morales, Jiménez-Estrada, & Mora-Escobedo, 2012; Mutungi et al., 2012).

Table 2
Structural characteristics determined by FTIR, XRD, LCM-Raman.

Varieties	IR ratio 1047/1022 cm^{-1}	IR ratio 1022/995 cm^{-1}	Relative crystallinity (%)	FWHH of the band at 480 cm^{-1}
NW1	0.86 ± 0.03a	1.01 ± 0.05a	38.7 ± 0.8a	14.3 ± 0.5a
TW1	0.87 ± 0.04a	0.96 ± 0.06a	39.6 ± 1.0a	14.3 ± 0.4a
YW1	0.90 ± 0.03a	0.95 ± 0.03a	40.0 ± 1.1a	14.5 ± 0.7a

Values are means ± SD. Means with similar letters in a column do not differ significantly ($p > 0.05$).
nd: not detected.
IR ratio determined by FTIR; relativity crystallinity determined by XRD; FWHH: full width at half height, determined by LCM-Raman.

The full width at half height (FWHH) has been used widely to characterize the structural variation of starch samples (Bulkin, Kwak, & Dea, 1987; Fechner, Wartewig, Kleinebudde, & Neubert, 2005; Mutungi et al., 2012). Band narrowing is an indicator for a narrower distribution of bond energies in the more ordered specimens (Bulkin et al., 1987). In general, the FWHH of starch samples declined in the band at 480 cm^{-1} with increasing starch crystallinity (Fechner et al., 2005; Mutungi et al., 2012). The FWHH of the band at 480 cm^{-1} was 14.3, 14.3 and 14.5 for NW1, TW1 and YW1 starches, respectively. No significant differences were noted between three waxy wheat starches, consistent with the XRD and FTIR results. XRD, FTIR and Raman results showed that three waxy wheat starches have similar relative crystallinity and short-range molecular order of double helices.

3.6. Swelling power

The swelling power was determined at the temperature ranging from 50 to 90 °C (Table 3). Swelling power increased with the increasing temperature when the temperature was below 80 °C. At 50 °C, which is below the onset temperature of starch gelatinization, swelling power of three waxy starches was in the range of 2.81–3.57 g/g. At sub-gelatinization temperature, starch granules can absorb small amount of water and swell to a very limited extent. With temperature increasing, water is increasingly absorbed into starch granules, resulting in the increasing swelling

Table 3
Functional properties of three waxy wheat starches.

Varieties	Functional properties					
Swelling power (g/g)						
	50 °C	60 °C	70 °C	80 °C	90 °C	
NW1	2.8 ± 0.8a	13.4 ± 0.6b	23.4 ± 0.6a	28.8 ± 0.7a	28.6 ± 0.5a	
TW1	3.6 ± 0.5a	12.3 ± 0.2a	23.9 ± 0.1a	28.5 ± 0.8a	28.7 ± 0.7a	
YW1	3.3 ± 1.2a	13.4 ± 0.3b	25.1 ± 0.2b	28.6 ± 0.6a	28.4 ± 0.7a	
Gelatinization						
	T_o (°C)	T_p (°C)	T_c (°C)	$T_c - T_o$ (°C)	ΔH (J/g)	
NW1	60.0 ± 0.1a	64.4 ± 0.1b	70.9 ± 0.1b	10.9 ± 0.1b	15.1 ± 0.1b	
TW1	61.3 ± 0.2b	65.9 ± 0.1c	72.2 ± 0.2c	10.9 ± 0.2b	14.8 ± 0.7ab	
YW1	60.0 ± 0.2a	64.1 ± 0.1a	69.7 ± 0.4a	9.7 ± 0.2a	13.9 ± 0.3a	
Retrogradation						
NW1	nd	nd	nd	nd	nd	
TW1	nd	nd	nd	nd	nd	
YW1	nd	nd	nd	nd	nd	
Pasting properties						
	PV (cp)	TV (cp)	FV (cp)	BD (cp)	SB (cp)	PT (°C)
NW1	4022 ± 37a	1378 ± 1a	1702 ± 38a	2644 ± 38a	324 ± 37a	67.4 ± 0.7a
TW1	4032 ± 6a	1372 ± 4a	1693 ± 7a	2668 ± 4a	329 ± 2a	68.7 ± 0.0a
YW1	4243 ± 2b	1413 ± 64a	1659 ± 1a	2830 ± 66b	246 ± 62a	67.0 ± 0.0a

Values are means ± SD. Means with similar letters in a column do not differ significantly ($p > 0.05$).
nd: not detected.
T_o: onset temperature; T_p: peak temperature; T_c: conclusion temperature; ΔH: enthalpy change.
PV: peak viscosity; TV: trough viscosity; FV: final viscosity; BD: breakdown; SB: setback; PT: pasting temperature.

power. In comparison, YW1 starch showed a bit higher swelling power than did two other waxy starches. When the temperature was at 80 °C or higher, waxy wheat starch granules can absorb all of the water added and form the soft gels. On centrifugation, no clear supernatant was obtained, indicative of the strong binding of water by the swollen amylopectin molecules (Wang, Li, Yu, Copeland, & Wang, 2014). In this regard, swelling power of three waxy wheat starches was about 28.5 g/g. The swelling power of native starch granules is primarily a property of amylopectin molecules. The small differences in swelling power of three waxy wheat starches suggested that little variability occurs in the fine structure of amylopectin molecules.

3.7. Gelatinization and retrogradation

The gelatinization parameters, including T_o, T_p, T_c, and enthalpy change (ΔH), were determined by differential scanning calorimetry (DSC) (Table 3). There were small, and in some cases significant, differences between the starches in gelatinization parameters. For example, the enthalpy change of three waxy wheat starches ranged from 13.9 to 15.1 J/g. The enthalpy changes of waxy wheat starches were higher than those reported for normal wheat starches (Yu et al., 2015). The DSC endothermic peak associated with starch gelatinization reflects the loss of ordered structures (double helices/crystallites) of starch granules (Cooke & Gidley, 1992). The small difference in ΔH of three waxy wheat starches is in general agreement with the similarity in relative crystallinity and molecular order of starch granules. At a water/starch ratio of 3:1, swelling of waxy starch granules is incomplete and endothermic transition reflects the partial swelling behavior of starch granules rather than full gelatinization (Wang & Copeland, 2012b; Wang, Li, et al., 2014). Hence, the ΔH during DSC heating under a water-limited condition does not fully reflect the crystallinity of starch granules (Wang, Li, et al., 2014). This may explain similar ordered structures of NW1 and YW1 starches leading to the small but significant differences in ΔH.

To investigate the retrogradation of waxy wheat starch gels, gelatinized waxy starch gels after DSC measurement were stored at 4 °C for 5 days. The stored waxy wheat starch gels did not show any endothermic transition from 20 to 120 °C, indicating that retrogradation of waxy wheat starch gel, from the viewpoint of long-range order, was too limited to be detected by DSC. In comparison with normal starch (Wang, Luo et al., 2014), waxy starch is less liable to retrograde, making waxy starch more suitable for the production of starch-based foods that needs to be stored at low temperature.

3.8. Pasting characteristics

Three waxy wheat starches presented the similar pasting profiles (data not shown). The pasting parameters derived from RVA profiles were slightly different between starches (Table 3). For example, no significant differences were observed in trough viscosity (1372–1413cp), final viscosity (1659–1702cp), setback viscosity (246–324cp), and pasting temperature (67.0–68.7 °C). For peak viscosity and breakdown viscosity, YW1 starch showed higher values than did NW1 and TW1 starches. In comparison with normal wheat starch (Yu et al., 2015), waxy wheat starch granules showed higher peak viscosity, lower setback viscosity and lower pasting temperature.

Peak viscosity of starch granules is thought to be related to swelling power. The higher peak viscosity of YW1 starch could be attributed to its higher swelling power as observed at 70 °C (Table 3). Additionally, the higher peak viscosity of YW1 could be related to the larger particle size (Table 1), which can bring about higher friction of swollen granules. Breakdown viscosity is a measure of stability of hot starch paste under the shear force. The higher breakdown of YW1 starch was indicative of lower stability of hot paste under shear force. The breakdown of hot starch paste viscosity is caused by shear-induced disruption of the swollen granules and leached starch components orienting themselves in the direction of stirring (Wang & Copeland, 2015). Granule size, shape, swelling capacity, and amylopectin structure can all affect the breakdown viscosity of starch granules (Han & Hamaker, 2001). The higher breakdown viscosity of YW1 starch could be related to its higher swelling power and greater mean particle size. The low and similar values of setback viscosity of three waxy wheat starches indicated that retrogradation of starch during RVA cooling

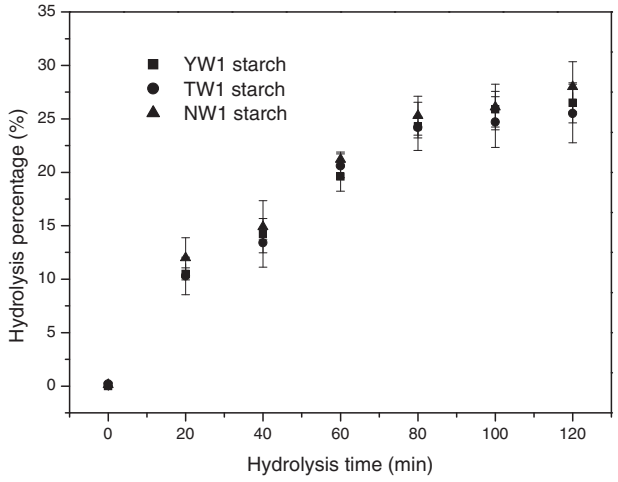

Fig. 3. The dynamic curves of *in vitro* enzymatic digestion of three waxy wheat starches.

occurs in a slow and similar rate compared to normal wheat starch (Wang, Li, et al., 2014). The low setback of three waxy wheat starches was consistent with the low retrogradation determined by DSC.

3.9. In vitro enzymatic digestibility

The dynamic curves of starch *in vitro* enzymatic digestion by porcine pancreatic α-amylase and amyloglucosidase at different time points are presented in Fig. 3. The hydrolysis percentage of three waxy wheat starches increased with time. Although small differences in hydrolysis percentage were observed between the starches at each time point, these differences were not significant. For example, the RDS content of three waxy starches was 12.0%, 10.3% and 10.5% for NW1, TW1 and YW1, respectively. Similarly, no significant differences were noted for SDS and RS content between the starches. Native starch granules differ significantly in their susceptibility to enzymatic digestion, with botanical origin being a major source of variability in digestibility. Native potato and high amylose starch are the most resistant to enzymatic digestion, whereas waxy starch is much more susceptible to enzymatic digestion than normal or higher amylose starches (Wang & Copeland, 2013). Granule size and surface characteristics (for example, pores, grooves or furrows, and surface-associated proteins and lipids), starch damage, amylose content, fine structure of amylopectin, degree of crystallinity and phosphorus content, can all affect native starch digestibility (Wang & Copeland, 2013). The small difference in enzymatic digestibility of three waxy maize starches could be attributed to the small variability of starch structural characteristics, as shown in Tables 1 and 2.

4. Conclusions

The molecular order and functional properties of starches from three waxy wheat varieties grown in China were characterized. Three waxy wheat starches, which were essentially free of amylose, exhibited similar granular morphology, average particle size, crystalline polymorphism, and long- and short-range ordered structures. There were small, and in some cases significant, differences in the functional properties of three waxy wheat starches, such as swelling power, gelatinization parameters, pasting viscosities and *in vitro* enzymatic digestibility. Waxy wheat starches showed very slow retrogradation, which make them more suitable for the incorporation of easily retrograded starch-based foods to regard the firming or staling of these foods.

Acknowledgements

The authors gratefully acknowledge the financial supports from the National Natural Science Foundation of China (31401651, 31371720) and the Natural Science Foundation of Tianjin (13JCYBJC38100). Shujun Wang also greatly appreciates the financial support of "Haihe Scholar Program" (000050401) and Tianjin "1000 Youth Talents Plan" from Tianjin University of Science & Technology. The authors would like to give special thanks to Lixiahe Agricultural Science Institute, Jiangsu Province, for providing the waxy wheat grains.

References

Bulkin, B. J., Kwak, Y., & Dea, I. C. M. (1987). Retrogradation kinetics of waxy-corn and potato starches-A rapid, Raman-spectroscopic study. *Carbohydrate Research, 160*, 95–112.
Chakraboty, M., Matkovic, K., Grier, D. G., Jarabek, E. L., Berzonsky, W. A., McMullen, M. S., et al. (2004). Physicochemical and functional properties of Tetraploid and Hexaploid waxy wheat starch. *Starch/Staerke, 56*, 339–347.
Chrastil, J. (1987). Improved colorimetric determination of amylose in starches or flours. *Carbohydrate Research, 159*, 154–158.
Cooke, D., & Gidley, M. J. (1992). Loss of crystalline and molecular order during starch gelatinization: Origin of the enthalpic transition. *Carbohydrate Research, 227*(6), 103–112.
Dodson, J. R., Li, X., Zhou, X., Zhao, K., Sun, N., & Atahan, P. (2013). Origin and spread of wheat in China. *Quaternary Science Reviews, 72*, 108–111.
Fannon, J. E., Hauber, R. J., & BeMiller, J. N. (1992). Surface pores of starch granules. *Cereal Chemistry, 69*, 284–288.
Flores-Morales, A., Jiménez-Estrada, M., & Mora-Escobedo, R. (2012). Determination of the structural changes by FT-IR, Raman, and CP/MAS ^{13}C NMR spectroscopy on retrograded starch of maize tortillas. *Carbohydrate Polymers, 87*, 61–68.
Fechner, P. M., Wartewig, S., Kleinebudde, P., & Neubert, R. N. H. (2005). Study of the retragradation process for various starch gel using Raman spectroscopy. *Carbohydrate Research, 340*, 2563–2568.
Fujita, S., Yamamoto, H., Sugimoto, Y., Morita, N., & Yamamori, M. (1998). Thermal and crystalline properties of waxy wheat (*Triticum aestivum L.*) starch. *Journal of Cereal Science, 27*, 1–5.
Goesaert, H., Brijs, K., Veraverbeke, W. S., Courtin, C. M., Gebruers, K., & Delcour, J. A. (2005). Wheat flour constituents: How they impact bread quality, and how to impact their functionality. *Trends in Food Science & Technology, 16*, 12–30.
Gidley, M. J. (1987). Factors affecting the crystalline type (A–C) of native starches and model compounds: A rationalization of observed effects in terms of polymorphic structures. *Carbohydrate Research, 161*, 301–304.
Hung, P. V., Maeda, T., & Morita, N. (2006). Waxy and high-amylose wheat starches and flours-characteristics, functionality and application. *Trends in Food Science & Technology, 17*, 448–456.
Han, X.-Z., & Hamaker, B. R. (2001). Amylopectin fine structure and rice starch paste breakdown. *Journal of Cereal Science, 34*, 279–284.
Kim, H.-S., & Huber, K. C. (2010). Physicochemical properties and amylopectin fine structures of A- and B-type granules of waxy and normal soft wheat starch. *Journal of Cereal Science, 51*, 256–264.
Kizil, R., Irudayaraj, J., & Seetharaman, K. (2002). Characterization of irradiated starch by using FT-Raman and FTIR spectroscopy. *Journal of Agricultural and Food Chemistry, 50*, 3912–3918.
Kumar, S. B., & Prabhasankar, P. (2014). Low glycemic index ingredients and modified starches in wheat based food processing: A review. *Trends in Food Science & Technology, 35*, 32–41.
Mutungi, C., Passauer, L., Onyango, C., Jaros, D., & Rohm, H. (2012). Debranched cassava starch crystallinity determination by Raman spectroscopy: Correlation of features in Raman spectra with X-ray diffraction and ^{13}C CP/MAS NMR spectroscopy. *Carbohydrate Polymers, 87*, 598–606.
Ma, H., Zhang, X., Wang, G., Gao, D., Zhang, B., Lv, G., et al. (2013). Effect of wx genes on amylose content, physicochemical properties of wheat starch, and the suitability of waxy genotype for producing Chinese crisp sticks. *Journal of Cereal Science, 58*, 140–147.
Man, J., Yang, Y., Zhang, C., Zhou, X., Dong, Y., Zhang, F., et al. (2012). Structural changes of high-amylose rice starch residues following in Vitro and in Vivo digestion. *Journal of Agricultural and Food Chemistry, 60*, 9332–9341.
Nakamura, T., Yamamori, M., Hirano, H., Hidaka, S., & Nagamine, T. (1995). Production of waxy (amylose-free) wheats. *Molecular Genetics and Genomics, 248*, 253–259.
Salman, H., Blazek, J., Lopez-Rubio, A., Gilbert, E. P., Hanley, T., & Copeland, L. (2009). Structure-function relationships in A and B granules from wheat starches. *Carbohydrate Polymers, 75*, 420–427.
Sevenou, O., Hill, S. E., Farhat, I. A., & Mitchell, J. R. (2002). Organisation of the external region of the starch granule as determined by infrared spectroscopy. *International Journal of Biological Macromolecules, 31*, 79–85.

Shingel, K. I. (2002). Determination of structural peculiarities of dexran, pullulan and irradiated pullulan by Fourier-transform IR spectroscopy. *Carbohydrate Research, 337*, 1445–1451.

Smits, A. L. M., Ruhnau, F. C., Wliegenthart, J. F. G., & van Soest, J. J. G. (1998). Ageing of starch based systems as observed with FT-IR and solid state NMR spectroscopy. *Starch/Staerke, 50*, 478–483.

Wang, S., & Copeland, L. (2012a). New insights into loss of swelling power and pasting profiles of acid hydrolyzed starch granules. *Starch/Staerke, 64*, 538–544.

Wang, S., & Copeland, L. (2012b). Phase transitions of pea starch over a wide range of water content. *Journal of Agricultural and Food Chemistry, 60*, 6439–6446.

Wang, S., & Copeland, L. (2013). Molecular disassembly of starch granules during gelatinization and its effect on starch digestibility: A review. *Food & Function, 4*, 1564–1580.

Wang, S., & Copeland, L. (2015). Effect of acid hydrolysis on starch structure and functionality: A review. *Critical Reviews in Food Science & Nutrition, 55*, 1079–1095.

Wang, S., Hassani, M. E., Crossett, B., & Copeland, L. (2013). Extraction and identification of internal granule proteins from waxy wheat starch. *Starch/Staerke, 65*, 186–190.

Wang, S., Li, C., Yu, J., Copeland, L., & Wang, S. (2014). Phase transition and swelling behaviour of different starch granules over a wide range of water content. *LWT – Food Science & Technology, 59*, 597–604.

Wang, S., Luo, H., Zhang, J., Zhang, Y., He, Z., & Wang, S. (2014). Alkali-induced changes in functional properties and in vitro digestibility of wheat starch: The role of surface proteins and lipids. *Journal of Agricultural and Food Chemistry, 62*, 3636–3643.

Wang, S., Sharp, P., & Copeland, L. (2011). Structural and functional properties of starches from field peas. *Food Chemistry, 126*, 1546–1552.

Wang, S., Yu, J., Zhu, Q., Yu, J., & Jin, F. (2009). Granular structure and allomorph position in C-type Chinese yam starch granule revealed by SEM, ^{13}C CP/MAS NMR and XRD. *Food Hydrocolloids, 23*, 426–433.

Yoo, S. H., & Jane, J. (2002). Structural and physical characteristics of waxy and other wheat starches. *Carbohydrate Polymers, 49*, 297–305.

Yu, J., Wang, S., Wang, J., Li, C., Xin, Q., Huang, W., et al. (2015). Effect of laboratory milling on properties of starches isolated from different flour millstreams of hard and soft wheat. *Food Chemistry, 172*, 504–514.

Zhang, H., Zhang, W., Xu, C., & Zhou, X. (2013). Morphological features and physicochemical properties of waxy wheat starch. *International Journal of Biological Macromolecules, 62*, 304–309.